nature microbiology

ARTICLES

https://doi.org/10.1038/s41564-022-01207-8

Multiple phage resistance systems inhibit infection via SIR2-dependent NAD$^+$ depletion

Jeremy Garb[1], Anna Lopatina[1,3], Aude Bernheim[1,4], Mindaugas Zaremba[2], Virginijus Siksnys[2], Sarah Melamed[1], Azita Leavitt[1], Adi Millman[1], Gil Amitai[1] and Rotem Sorek[1]✉

Defence-associated sirtuins (DSRs) comprise a family of proteins that defend bacteria from phage infection via an unknown mechanism. These proteins are common in bacteria and harbour an N-terminal sirtuin (SIR2) domain. In this study we report that DSR proteins degrade nicotinamide adenine dinucleotide (NAD$^+$) during infection, depleting the cell of this essential molecule and aborting phage propagation. Our data show that one of these proteins, DSR2, directly identifies phage tail tube proteins and then becomes an active NADase in *Bacillus subtilis*. Using a phage mating methodology that promotes genetic exchange between pairs of DSR2-sensitive and DSR2–resistant phages, we further show that some phages express anti-DSR2 proteins that bind and repress DSR2. Finally, we demonstrate that the SIR2 domain serves as an effector NADase in a diverse set of phage defence systems outside the DSR family. Our results establish the general role of SIR2 domains in bacterial immunity against phages.

Sirtuin (SIR2)-domain proteins are found in organisms ranging from bacteria to humans. These proteins have been widely studied in yeast and mammals, where they were shown to regulate transcription repression, recombination, DNA repair and cell-cycle processes[1]. In eukaryotes, SIR2 domains were shown to possess enzymatic activities, and function either as protein deacetylases or ADP ribosyltransferases[2,3]. In both cases, the SIR2 domain utilizes nicotinamide adenine dinucleotide (NAD$^+$) as a cofactor for the enzymatic reaction[4].

In bacteria, SIR2 domains were recently shown to participate in defence systems that protect against phages. These domains are associated with multiple different defence systems, including prokaryotic argonautes (pAgo)[5], Thoeris[6,7], AVAST, defence-associated sirtuin (DSR) and additional systems[8]. It was recently shown that the SIR2 domain in the Thoeris defence system is an NADase responsible for depleting NAD$^+$ from the cell once phage infection has been sensed[7]. However, it is currently unknown whether SIR2 domains in other defence systems perform a similar function or whether they have other roles in phage defence.

Results

DSR2 defends against phage SPR via abortive infection. To study the role of SIR2 domains in bacterial anti-phage defence, we began by focusing on DSR2, a minimal defence system that includes a single protein with an N-terminal SIR2 domain and no additional identifiable domains (Fig. 1a). The DSR2 gene family was recently identified based on a screen for genes commonly found in bacterial anti-phage defence islands[8]. We cloned the DSR2 gene from *Bacillus subtilis* 29R, under the control of its native promoter, into the genome of *B. subtilis* BEST7003 which naturally lacks this gene, and challenged the DSR2-containing strain with a set of phages from the SPbeta family. We found that DSR2 protected *B. subtilis* against phage SPR, reducing plating efficiency by four orders of magnitude (Fig. 1b and Extended Data Fig. 1). Point mutations in residues N133 and H171 in DSR2, both of which predicted to disable the active site of the SIR2 domain, abolished defence, suggesting that the enzymatic activity of SIR2 is essential for DSR2 defence (Fig. 1b).

We next tested whether DSR2 defends via abortive infection, a process that involves premature death or growth arrest of the infected cell, preventing phage replication and spread to nearby cells[9]. When infected in liquid media, DSR2-containing bacterial cultures collapsed if the culture was infected by phage in high multiplicity of infection (MOI), similar to DSR2-lacking cells (Fig. 1c). However, despite collapsing the culture, phages were not able to replicate on DSR2-containing cells (Extended Data Fig. 2). In low MOI infection, DSR2-lacking control cultures collapsed but DSR2-containing bacteria survived (Fig. 1c). This phenotype is a hallmark of abortive infection, in which infected bacteria that contain the defence system do not survive but also do not produce phage progeny[9].

DSR2 depletes NAD$^+$ upon phage infection. To ask whether DSR2 manipulates the NAD$^+$ content of the cell during phage infection, we used mass spectrometry to monitor NAD$^+$ levels in infected cells at various time points following initial infection. When DSR2-containing cells were infected by phage SPR, cellular NAD$^+$ decreased sharply between 20 and 30 min from the onset of infection (Fig. 1d). NAD$^+$ levels did not change in cells in which the SIR2 active site was mutated, or in DSR2-lacking control cells, suggesting that the SIR2 domain is responsible for the observed NAD$^+$ depletion (Fig. 1d). In parallel with NAD$^+$ depletion, we observed accumulation of the product of NAD$^+$ cleavage, ADP-ribose (ADPR) (Fig. 1e). These results demonstrate that DSR2 is an abortive infection protein that causes NAD$^+$ depletion in infected cells.

DSR2 strongly protected *B. subtilis* cells against SPR, a phage belonging to the SPbeta group of phages[10] (Fig. 1b and Extended Data Fig. 1). However, the defence gene failed to protect against phages phi3T and SPbeta, although both these phages belong to the same phage group as SPR (Fig. 1b). This observation suggests that phages phi3T and SPbeta either encode genes that inhibit DSR2, or

[1]Department of Molecular Genetics, Weizmann Institute of Science, Rehovot, Israel. [2]Institute of Biotechnology, Life Sciences Center, Vilnius University, Vilnius, Lithuania. [3]Present address: Division of Microbial Ecology, Center for Microbiology and Environmental Systems Science, University of Vienna, Vienna, Austria. [4]Present address: SEED, U1284, INSERM, Université Paris Cité, Paris, France. ✉e-mail: rotem.sorek@weizmann.ac.il

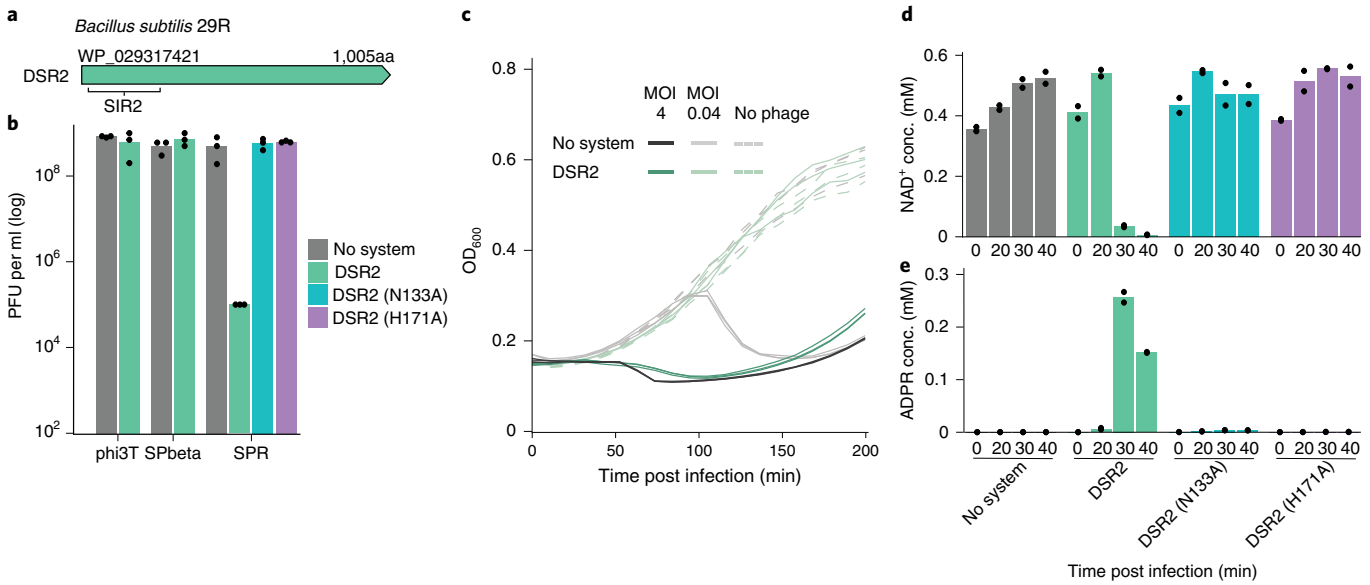

Fig. 1 | DSR2 is an abortive infection protein that causes NAD$^+$ depletion in infected cells. a, Domain organization of DSR2 from *B. subtilis* 29R. Protein accession in NCBI is indicated above the gene. **b**, Efficiency of plating (EOP) for three phages infecting the control *B. subtilis* BEST7003 strain (no system) or *B. subtilis* BEST7003 with DSR2 cloned from *B. subtilis* 29R. For phage SPR, EOP is also presented for two mutations in the predicted SIR2 catalytic site. Data represent plaque-forming units (PFU) per millilitre. Bar graphs represent average of three independent replicates, with individual data points overlaid. **c**, Liquid culture growth of DSR2-containing *B. subtilis* and control *B. subtilis* (no system), infected by phage SPR at 30 °C. Bacteria were infected at time 0 at an MOI of 4 or 0.04. Three independent replicates are shown for each MOI, and each curve represents an individual replicate. **d**,**e**, Concentrations (conc.) of NAD$^+$ (**d**) and ADPR (**e**) in cell lysates extracted from SPR-infected cells as measured by targeted LC-MS with synthesized standards. The *x* axis represents minutes post infection, with zero representing non-infected cells. Cells were infected by phage SPR at an MOI of 5 at 30 °C. Bar graphs represent the average of two biological replicates, with individual data points overlaid. Colours are as in **b**.

lack genes that are recognized by DSR2 and trigger its NADase activity. The phages SPR, phi3T and SPbeta all share substantial genomic regions with high sequence homology (Fig. 2a). We therefore reasoned that co-infecting cells with two phages, either SPR and phi3T, or SPR and SPbeta, may result in recombination-mediated genetic exchange between the phages, which would enable pinpointing genes that allow escape from DSR2 defence when acquired by SPR (Fig. 2b). Such crossing techniques were previously successful in pinpointing genetic phenotypes in phages[11,12].

To generate a bacterial host that would select for such genetic exchange events, we cloned into DSR2-containing cells an additional defence protein, a prokaryotic viperin homologue (pVip) from *Fibrobacter* sp. UWT3 (ref. [13]). The pVip protein, when expressed alone in *B. subtilis*, protected it from phi3T and SPbeta but not from SPR, a defence profile opposite to that of the DSR2 profile in terms of the affected phages (Extended Data Fig. 3). Accordingly, none of the three SPbeta-group phages could form plaques on the strain that expressed both defensive genes. However, when simultaneously infecting the double defence strain with SPR and either phi3T or SPbeta, plaque-forming hybrids were readily obtained, indicating that these hybrid phages recombined and acquired a combination of genes enabling their escape from both DSR2 and pVip (Fig. 2c).

A phage-encoded anti-DSR2 protein. We isolated and sequenced 32 such hybrid phages, assembled their genomes and compared these genomes with the genome of the parent SPR phage (Fig. 2d and Supplementary File 1). This led to the identification of two genomic segments that were repeatedly acquired by SPR phages. Acquisition of either of these segments from a genome of a co-infecting phage rendered SPR resistant to DSR2 (Fig. 2d). The first segment included five small genes of unknown function present in phages phi3T and SPbeta but not in the wild-type SPR phage, and we therefore tested whether any of these genes were capable of inhibiting DSR2. One of the genes, when co-expressed with DSR2, rendered DSR2 inactive, suggesting that this phage gene encodes an anti-DSR2 protein (Fig. 3a). The other four genes in the segment did not inhibit DSR2 defence (Extended Data Fig. 4a). The DSR2-inhibiting protein, which we named DSAD1 (DSR anti-defence 1), is 120 amino acids long and has no identifiable sequence homology to proteins of known function. Co-expression of DSR2 and tagged DSAD1, followed by pulldown assays, showed direct interaction between the two proteins (Fig. 3b). These results indicate that DSAD1 is a phage protein that binds and inhibits DSR2.

DSR2 is activated by phage tail tube protein. We next examined the second genomic segment that, when acquired, allowed phage hybrids to escape DSR2. In the parent SPR phage, this region spans three operons encoding a set of phage structural proteins, including capsid and tail proteins. Hybrid phages in which the original genes were replaced by their homologues from SPbeta or phi3T become resistant to DSR2 (Fig. 2d). We hypothesized that one of the structural proteins in phage SPR is recognized by DSR2 to activate its defence, and when this protein is replaced by its homologue from another phage, recognition no longer occurs. To test this hypothesis, we attempted to clone each of the three operons found in the original DNA segment in SPR into *B. subtilis* cells that also express DSR2. One of these operons could not be cloned into DSR2-expressing cells, and we then repeated the cloning attempt for each of the genes in the operon. One of these genes, encoding a tail tube protein, could not be cloned into DSR2-expressing cells but was readily cloned into cells in which the DSR2 active site was mutated (Fig. 3c and Extended Data Fig. 4b,c).

To further test if co-expression of DSR2 and the SPR tail tube protein is toxic to bacteria, we cloned each of these genes under an inducible promoter within *Escherichia coli* cells. In support of our hypothesis, growth was rapidly arrested in cells in which the

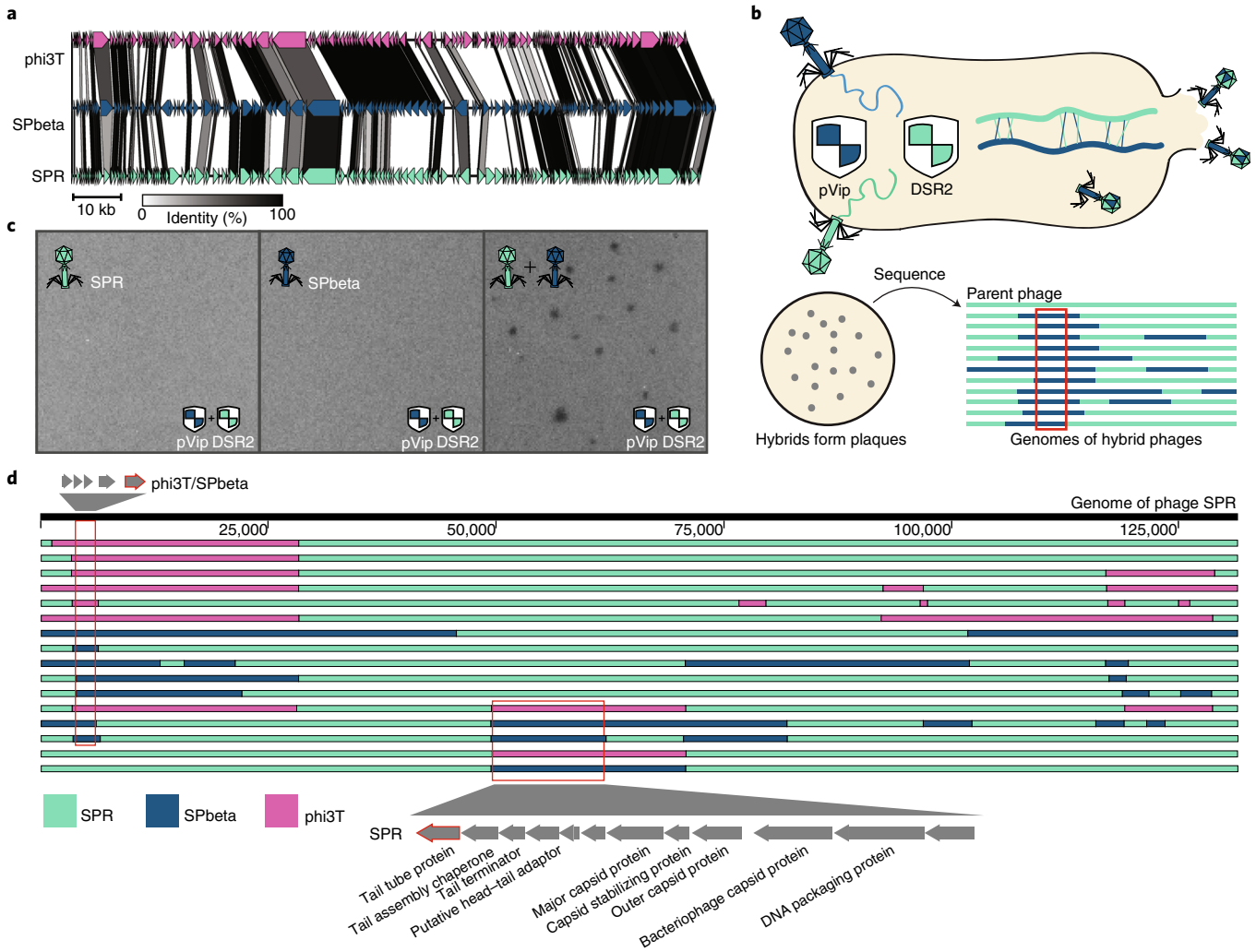

Fig. 2 | Genetic exchange between phages reveal regions responsible for escape from DSR2. a, Genome comparison of phages SPR, SPbeta and phi3T was performed using clinker[29]. Grey/black bands connect homologous genes, with shades of grey representing the percentage of amino-acid sequence identity. **b**, Schematic representation of the phage mating experiment. *B. subtilis* BEST7003 cells expressing both DSR2 and pVip are co-infected with phage SPR and SPbeta (or phi3T). Recombination between co-infecting phage genomes leads to hybrid phages that can overcome both defence systems and generate plaques. Examination of the genomes of multiple hybrids predicts genomic regions necessary to overcome defence. **c**, Plaque assays with either one or two co-infecting phages. Cells expressing both DSR2 and pVip are infected either with phage SPR (left), phage SPbeta (middle) or both phages (right). **d**, Hybrid phage genomes. Each horizontal line represents the genome of a hybrid phage that can overcome DSR2. Green areas are from phage SPR, blue from SPbeta and purple from phi3T. Representative non-redundant hybrid sequences are presented out of 32 sequenced hybrids. Red rectangles outline two areas that are predicted to allow the phage to overcome DSR2 defence. The top enlarged inset shows genes found in the region acquired from phi3T or SPbeta; the gene outlined in red codes for DSAD1. The bottom enlarged inset shows genes present in the original SPR genome; the outlined gene is the tail tube protein.

expression of both genes was induced (Fig. 3d), and these cells became depleted of NAD$^+$ (Fig. 3e,f). Furthermore, pulldown assays with tagged proteins showed that DSR2 directly binds the tail tube protein of phage SPR (Fig. 3b). The tail tube protein was not able to pull down DSR2 when DSAD1 was co-expressed in the same cells, suggesting that the tail tube protein and DSAD1 are competitive binders for DSR2 (Extended Data Fig. 5). These results demonstrate that the tail tube protein of phage SPR is directly recognized by the defence protein DSR2, and that this recognition triggers the NADase activity of DSR2 and results in growth arrest (Fig. 3g).

The original tail tube protein of phage SPR is substantially divergent from its counterparts from phages SPbeta or phi3T, sharing only ~40% amino-acid sequence identity with these proteins (Extended Data Fig. 6). This divergence explains why the replacement of the original SPR protein with its SPbeta homologue renders the hybrid phage resistant to DSR2. In support of this, the tail tube protein of phage SPbeta showed much weaker ability to pull down DSR2 as compared to the tail tube counterpart from phage SPR (Fig. 3b). Presumably, the evolutionary pressure imposed by DSR2 and other bacterial defence systems that recognize tail tube proteins has led to the observed diversification in these proteins in phages of the SPbeta group.

Various defence systems with SIR2 domains deplete NAD$^+$ upon infection. Our results show that DSR2 exerts its defensive activity by depleting NAD$^+$ from infected cells. NADase activity was also recently described in the Thoeris defence system, in which a small molecule signal activates a SIR2-encoding effector to deplete NAD$^+$ once phage infection has been recognized[7]. To test if NAD$^+$ depletion is a general activity of SIR2 domains in bacterial defence systems, we examined three additional defence systems that

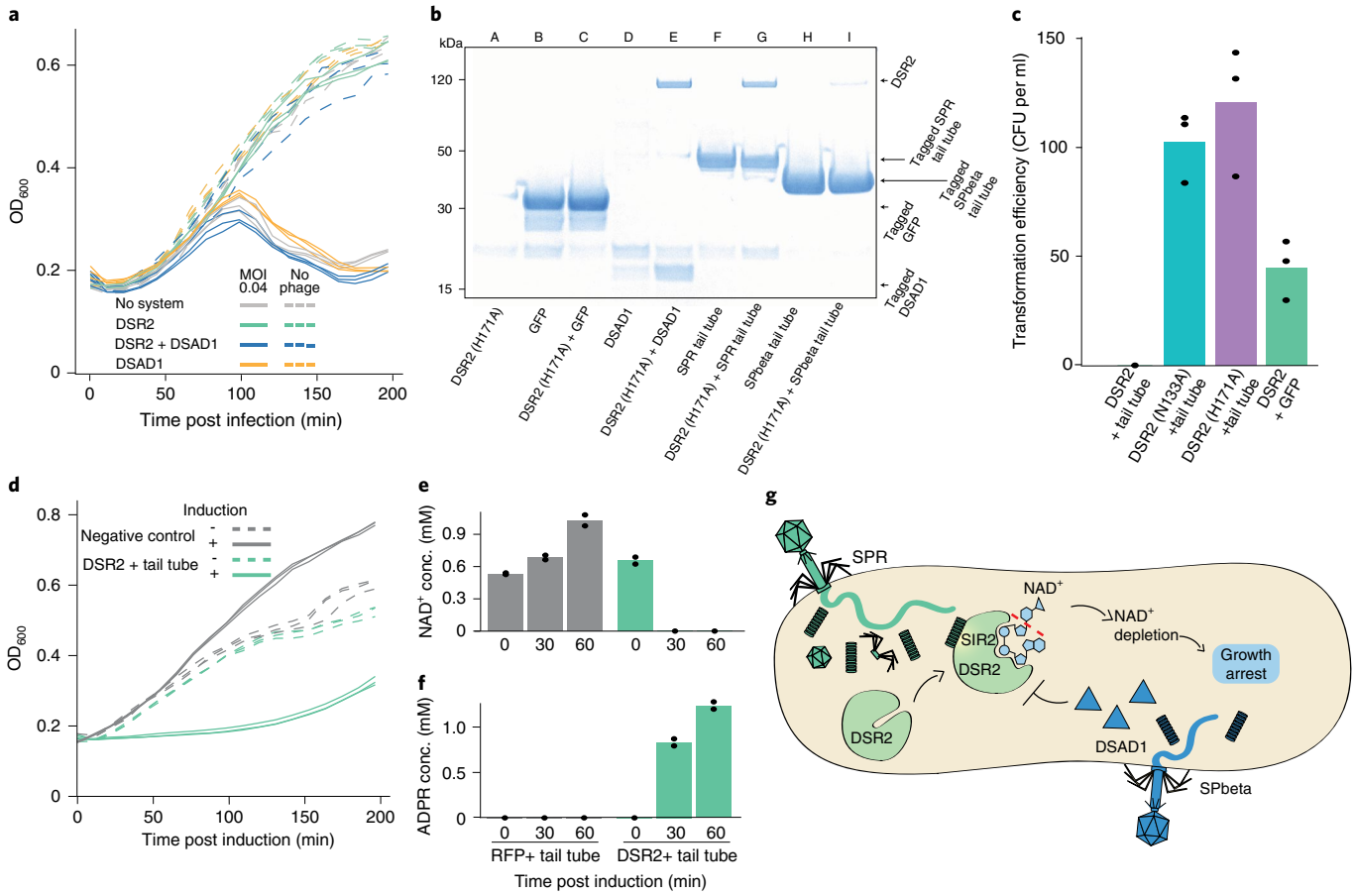

Fig. 3 | Phage proteins that activate and inhibit DSR2. a, DSAD1 inhibits DSR2 defence. Liquid culture growth of *B. subtilis* BEST7003 cells expressing either DSR2 alone, DSAD1 alone, or DSR2 and DSAD1, or control cells expressing neither gene, infected by phage SPR at 30 °C. Three independent replicates are shown. **b**, Pulldown assays of the DSR2-DSAD1 and DSR2-tail tube complexes. DSAD1, the tail tube proteins and control GFP were C-terminally tagged and co-expressed with DSR2. DSR2 in this experiment was mutated (H171A) to avoid toxicity. Shown is an SDS–PAGE gel. **c**, Transformation efficiencies of a vector containing the SPR tail tube protein or GFP control were measured for cells containing either WT DSR2 or two inactive DSR2 mutants. The *y* axis represents the number of colony-forming units (CFU) per millilitre. Bar graphs represent the average of three replicates, with individual data points overlaid. **d**, Liquid culture growth of *E. coli* that contains DSR2 and the tail tube gene of phage SPR, each under the control of an inducible promoter, and control *E. coli* that contains inducible GFP and DSR2 genes. Expression of both genes was induced at time 0. Three independent replicates are shown. **e**,**f**, Concentrations of NAD$^+$ (**e**) and ADPR (**f**) in cell lysates extracted from *E. coli* co-expressing DSR2 and SPR tail tube. The *x* axis represents minutes after expression induction, with zero representing non-induced cells. Control cells in this experiment express RFP and DSR2. Bar graphs represent the average of two biological replicates, with individual data points overlaid. **g**, A model for the mechanism of action of DSR2. Phage infection is sensed by the recognition of the phage tail tube protein through direct binding to DSR2. This triggers the enzymatic activity of the SIR2 domain to deplete the cell of NAD$^+$ thereby causing abortive infection. The phage anti-DSR2 protein DSAD1 inhibits DSR2 by direct binding.

contain a SIR2 domain (Fig. 4a). These systems included a two-gene system that encodes, in addition to the SIR2 domain, also a prokaryotic argonaute homologue (pAgo), a two-gene system that encodes a HerA-like DNA translocase[8], and a single SIR2-domain protein called DSR1[8] (Fig. 4a). DSR1 was cloned into *B. subtilis* BEST7003, while the other two systems were cloned into an *E. coli* host. Consistent with our hypothesis, these systems defended against multiple different phages (Fig. 4b and Extended Data Fig. 7), and NAD$^+$ depletion was observed in each case (Fig. 4c–e). Mutations inactivating the HerA-like DNA translocase or the pAgo protein abolished defence, indicating that these two proteins also participate in the defensive function (Extended Data Fig. 8). Liquid infection with high and low MOIs showed a phenotype consistent with abortive infection for the SIR2/pAgo and the SIR2-HerA systems (Fig. 4f,g). However, the DSR1 protein seems to inhibit the replication of phage phi29 without arresting the growth of the bacterial cells, and depletion of NAD$^+$ was only transient (Fig. 4e,h). Together, these results demonstrate a general role of SIR2 domains as NAD$^+$-depleting effectors in bacterial defence against phage.

Discussion

Our data suggest that NAD$^+$ depletion is a canonical function for SIR2 domains within bacterial defence systems. We show that four anti-phage defence systems, all containing SIR2 domains but otherwise comprising different architectures, deplete NAD$^+$ in response to phage infection. Specifically, in the case of DSR2, we show that this protein recognizes newly translated phage tail tube proteins to become an active NADase. Phages of the SPbeta family have at least two versions of the tail tube protein, and only certain alleles are strongly recognized by DSR2. In addition, we found that some phages in this family carry a small protein, DSAD1, which binds and inactivates DSR2.

NAD$^+$ depletion was previously shown to be toxic to bacterial cells[14–17], and it was recently demonstrated in the Thoeris, CBASS

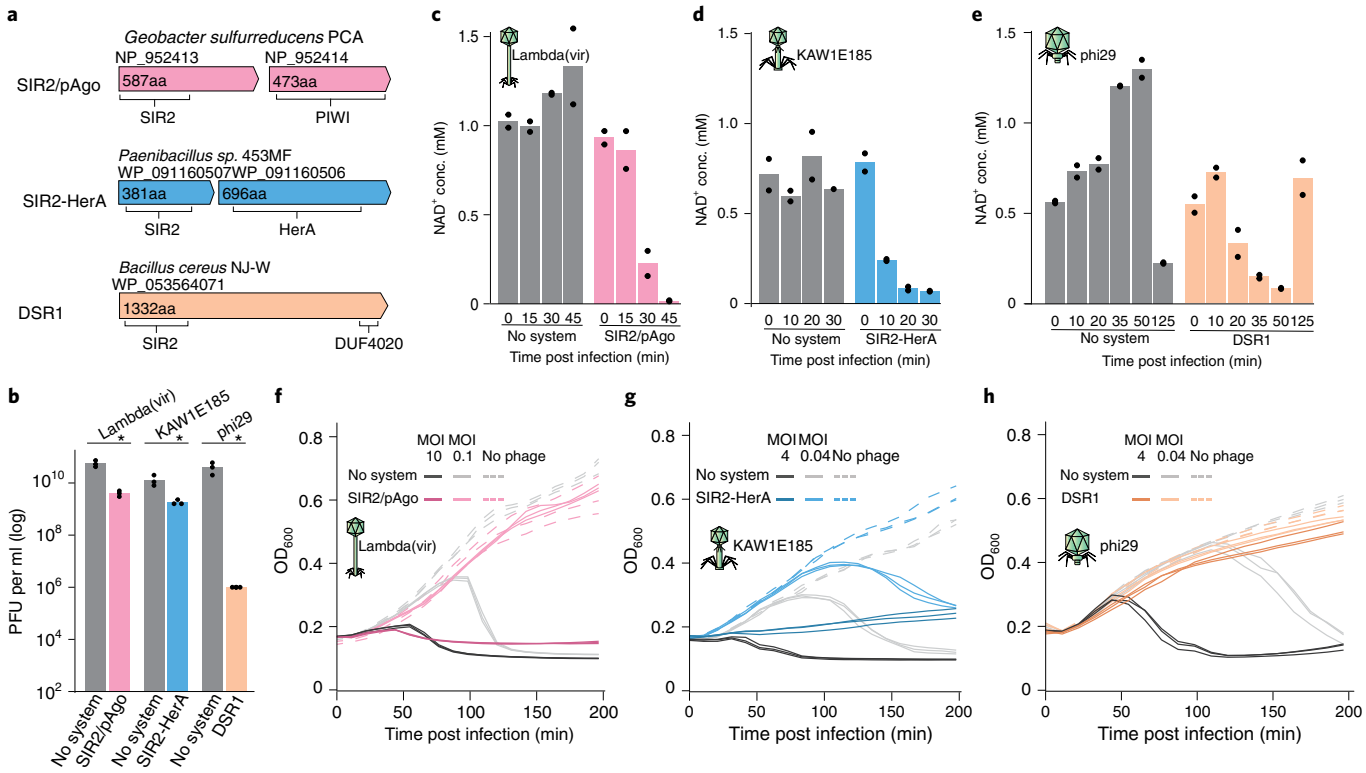

Fig. 4 | SIR2-containing defence systems deplete NAD⁺ in infected cells. a, Domain organization of three defence systems that contain SIR2 domains. Protein accessions in NCBI are indicated. **b**, Efficiency of plating for phages infecting defence-system-containing strains and control strains. SIR2-HerA and SIR2/pAgo were cloned into *E. coli* MG1655, and DSR1 was cloned into *B. subtilis* BEST7003. Bar graphs are the average of three biological replicates, with individual data points overlaid. KAW1E185 is short for vB_EcoM-KAW1E185, a T4-like phage. Asterisk marks statistically significant decrease (Student's *t*-test, two-sided, *P* values = 0.005, 0.036, 0.025, for phages lambda (vir), KAW1E185 and phi29, respectively). **c**–**e**, Concentrations of NAD⁺ in cell lysates extracted from infected SIR2-pAgo (**c**), SIR2-HerA (**d**) and DSR1 (**e**) cells as measured by targeted LC-MS with synthesized standards. The *x* axis represents minutes postinfection, with zero representing non-infected cells. 'No system' are control cells that contain an empty vector instead of the defence system. Bar graphs represent the average of two biological replicates, with individual data points overlaid. **f**–**h**, Liquid culture growth of bacteria contain the SIR2-pAgo (**f**), SIR2-HerA (**g**) or DSR1 (**h**) defence system and control bacteria contain an empty vector (no system). Bacteria were infected at time 0 at low or high MOIs, as indicated. Three independent replicates are shown for each MOI, and each curve shows an individual replicate.

and Pycsar systems that defence involving NAD⁺ depletion during phage infection is associated with an eventual cell death[7,15,18]. Indeed, in three out of the four SIR2-containing systems that we studied, growth arrest or death of the bacterial host was observed in response to phage infection. However, DSR1 protection from phage phi29 did not involve culture collapse (Fig. 4h). Furthermore, our data show that the NAD⁺ levels in cells containing DSR1 recovered after the initial depletion (Fig. 4e). It is possible that in some cases, reversible reduction of NAD⁺ to low but not zero levels may be enough to interfere with phage replication while still allowing cell growth. Alternatively, lowered levels of NAD⁺ might have different outcomes for the infected cell depending on additional components derived from the infecting phage.

The molecular signatures recognized by abortive infection defence systems as an indication for phage infection have been notoriously challenging to discover. In a minority of cases where the trigger was discovered, it was shown that some systems 'guard' an immunity hub in the cell, and become triggered when the phage tampers with the immunity complex[19,20]. In other cases, a specific protein expressed by the phage during infection forms the trigger for system activation, as shown for the *Staphylococcus* Stk2 abortive infection kinase[21], and also as we show for DSR2 in the current study. However, the SPR tail tube protein that activates DSR2 does not activate DSR1, suggesting that these two proteins recognize different molecular signatures (Extended Data Fig. 9). The mechanism by which phages activate, and potentially inhibit, the other three SIR2-domain-containing systems described in this study remains to be elucidated by future studies.

The arsenal of defence mechanisms known to protect bacteria against phage has recently been substantially expanded following the discovery of dozens of new anti-phage defence systems[6,8,22]. While the mechanism of defence was deciphered for some of these systems[7,13,18,23], in many cases it is not known what molecular patterns of the phage trigger these systems to become active. In the current study we used a 'phage mating' technique, which was previously successfully used in other studies[11,12], to promote genetic exchange between phages sensitive to the defence system and phages that can overcome it. Genome analyses of hybrid phages enabled us to pinpoint the exact phage proteins that activate or repress DSR2. We believe that the phage mating approach should be a useful tool for other studies attempting to identify phage triggers of bacterial defence systems.

Methods

Bacterial strains and phages. *B. subtilis* strain BEST7003 (obtained from I. Mitsuhiro at Keio University, Japan) was grown in MMB (lysogeny broth (LB) + 0.1 mM $MnCl_2$ + 5 mM $MgCl_2$, with or without 0.5% agar) at 30 °C. Whenever applicable, media were supplemented with spectinomycin (100 μg ml^{-1}) and chloramphenicol (5 μg ml^{-1}), to ensure selection of transformed and integrated cells. *E. coli* strain MG1655 (ATCC 47076) was grown in MMB at 37 °C. Whenever applicable, media were supplemented with ampicillin (100 μg ml^{-1}) or

Table 1 | Phages used in this study

Phage	Source	Identifier	Accession code
lambda(vir)	Udi Qimron		NC_001416.1
phi105	*Bacillus* Genetic Stock Centre (BGSC)	BGSC (1L11)	HM072038.1
phi29	Deutsche Sammlung von Mikroorganismen und Zellkulturen (DSMZ)	DSM 5546	NC_011048.1
phi3T	*Bacillus* Genetic Stock Centre (BGSC)	BGSC (1L1)	KY030782.1
SECphi17	Doron et al.[6]		LT960607.1
SECphi18	Doron et al.[6]		LT960609.1
SPbeta	*Bacillus* Genetic Stock Centre (BGSC)	BGSC (1L5)	AF020713.1
SPO1	Deutsche Sammlung von Mikroorganismen und Zellkulturen (DSMZ)	BGSC (1P4)	NC_011421.1
Spp1	Deutsche Sammlung von Mikroorganismen und Zellkulturen (DSMZ)	BGSC (1P7)	NC_004166.2
SPR	*Bacillus* Genetic Stock Centre (BGSC)	BGSC (1L56)	
T7	Udi Qimron		NC_001604.1
vB_EcoM-KAW1E185	Deutsche Sammlung von Mikroorganismen und Zellkulturen (DSMZ)	DSM 104099	NC_054922.1

Table 2 | SIR2-containing defence systems tested in this study

System	Host strain	Negative control	Phages used for MS and liquid growth assays	Phages used for infection plaque assays	Temperature (°C)	Induction
DSR2	*B. subtilis*	Empty cassette	SPR	phi29, spp1, SPR, SPbeta, phi3T, SPO1, phi105	30	Native promoter
DSR1	*B. subtilis*	Empty cassette	phi29	phi29, spp1, SPR, SPbeta, phi3T, SPO1, phi105	30	Native promoter
SIR2/ PAGO	*E. coli*	Empty pBAD	lambda(vir)	vB_EcoM-KAW1E185, lambda(vir), SECphi18, T7, SECphi17	37	0.2% arabinose
SIR2-HERA	*E. coli*	Empty vector	vB_EcoM-KAW1E185	vB_EcoM-KAW1E185, lambda(vir), SECphi18, T7, SECphi17	37	Native promoter

chloramphenicol (30 μg ml^{-1}) or kanamycin (50 μg ml^{-1}), to ensure the maintenance of plasmids. Phages used in this study are listed in Table 1.

Plasmid and strain construction. Details on defence systems analysed in this study are summarized in Table 2, and sequences of primers used in this study are in Supplementary Table 3. Defence systems DSR1, DSR2 and SIR2-HerA were synthesized by Genscript Corp. and cloned into the pSG1 plasmid[6] together with their native promoters. A whole operon of the SIR2/pAgo system, composed of the genes encoding the SIR2 (GSU1360, NP_952413.1) and pAgo (GSU1361, NP_952414.1) proteins, was amplified by PCR using the oligonucleotides MZ239 and MZ240, respectively, from the genomic DNA of *Geobacter sulfurreducens* Caccavo (LGC Standards catalogue no. 51573D-5). The resulting DNA fragment was digested by Eco31I (ThermoFisher catalogue no. FD0293) and XhoI (ThermoFisher catalogue no. FD0694) and using T4 DNA ligase (ThermoFisher catalogue no. EL0014) was cloned into pBAD/HisA expression vector (ThermoFisher catalogue no. V43001) precleaved with NheI (ThermoFisher catalogue no. FD0973) and XhoI and dephosphorylated using FastAP (ThermoFisher catalogue no. EF0651). The GsSir2 protein contains a His_6-Tag at its N terminus. The mutants DSR2 (N133A) and DSR2 (H171A) were constructed using the Q5 Site-directed Mutagenesis kit (NEB, E0554S) using either primers JG216 and JG217 or JG220 and JG221, respectively. The mutant DSR1 (H194A) was constructed using the Q5 Site-directed Mutagenesis kit using primers JG496 and JG497. The mutant SIR2-HerA (SIR2 D165A H212A) was constructed by first using the Q5 Site-directed Mutagenesis kit using primers JG498 and JG499 to introduce the D165A mutation, then using the resulting plasmid for further Q5 Site-directed Mutagenesis and the introduction of the second H212A mutation using primers JG500 and JG501. The mutant SIR2-HerA (HerA K167A) was constructed using the Q5 Site-directed Mutagenesis kit using primers JG502 and JG503. The mutant SIR2/pAgo (SIR2 N142A) was constructed using the Q5 Site-directed Mutagenesis kit using primers JG463 and JG464.To inactivate the GsAgo protein a bulky His_6-StrepII-His_6-tag (HSH tag, 29 amino acids: LEGHHHHHHSSWSHPQFEKGVEGHHHHHH) was fused to its C terminus. For this, a whole operon of the GsSir2/Ago system was amplified by PCR using the oligonucleotides MZ-325 and MZ-326, respectively, from the genomic DNA. The resulting DNA fragment was digested by Eco31I and XhoI and using T4 DNA ligase was cloned into pBAD24-HSH expression vector precleaved with NcoI (ThermoFisher catalogue no. FD0573) and XhoI and dephosphorylated using FastAP. In this case, the GsSir2 protein does not contain any tag at its N terminus.

A cloning shuttle vector for large fragments was constructed by Genscript Corp. This vector was constructed by replacing the Pxyl promoter and its downstream open reading frame in plasmid pGO1_thrC_Pxyl_cereus_ThsA[7], with a synthesized Phspank sfGFP cassette taken from pDR111 (ref. [24]), resulting in the plasmid pSG-thrC_Phspank_sfGFP (Supplementary File 2). The vector contains a p15a origin of replication and ampicillin resistance for plasmid propagation in *E. coli*, and a thrC integration cassette with chloramphenicol resistance for genomic integration into *B. subtilis*.

DSAD1 from SPbeta (National Center for Biotechnology Information (NCBI) protein accession WP_004399562) and phage tail tube protein from SPR (NCBI protein accession WP_010328117) were amplified from phage genomic DNA using primers JG346 and JG347 (for DSAD1) and JG142 and JG143 (for tail tube), and cloned into the pSG-thrC_Phspank_sfGFP vector, replacing sfGFP. The vector backbone was amplified using primers JG13 and JG14.

The additional DSR2 activator candidates tested in this research were also amplified from phage SPR genomic DNA and cloned into the pSG-thrC_Phspank_sfGFP vector, replacing sfGFP. 'Operon 1' was lifted with JG431 and J432. 'Operon 2' was lifted with JG433 and JG434. 'Operon 3' was lifted with JG435 and JG436. 'gene 5' was lifted with JG437 and JG438. 'gene 6' was lifted with JG439 and JG440. 'gene 7' was lifted with JG441 and JG442.

In a similar fashion, the additional DSR2 inhibition candidates tested in this paper were amplified from phage SPbeta. 'gene 1' was lifted with JG134 and JG183. 'gene 2' was lifted with JG184 and JG185. 'gene 3' was lifted with JG186 and JG187. 'gene 4' was lifted with JG188 and JG189.

For expression in *E. coli MG1655*, DSR2 and DSR2(H171A) were amplified and cloned into the plasmid pBbA6c-RFP (Addgene, catalogue no. 35290) using primers JG259 and JG260. The SPR tail tube gene was amplified from phage genomic DNA and cloned into the plasmid pBbS8k-RFP (Addgene, catalogue no. 35276) with primers JG249 and JG250 for inducible expression in *E. coli*.

For the assembly of tagged protein constructs, a pBbS8k with sfGFP fused to a C-terminal TwinStrep tag was first constructed (Supplementary File 3). The pBbS8k vector backbone was amplified using primers JG406 and JG407, and the sfGFP with a C-terminal TwinStrep tag was amplified from an *amyE* shuttle vector pGO6_amyE_hspank_GFP[7] with primers JG366 and JG367 and cloned into the pBbS8k plasmid, replacing RFP. To create the C-terminally tagged SPR tail tube, SPbeta tail tube and DSAD1 constructs, the genes were amplified from phage genomic DNA using primers JG408 and JG409 (for SPR tail tube), JG421 and JG422 (for SPbeta tail tube) and JG410 and JG411 (for DSAD1) and cloned into the pBbS8k sfGFP with C-terminal TwinStrep mentioned above, replacing sfGFP. For this, the pBbS8k with C-terminal TwinStrep vector backbone was amplified using primers JG407 and JG412.

For the assembly of a DSAD1-gene-containing plasmid, compatible with both pBbS8k and pBbA6c, the DSAD1 gene was lifted from phage SPbeta genomic DNA using primers JG429 and JG430 and Gibson assembled with a backbone amplified

from plasmid pAraGFPCDF (Addgene, catalogue no. 47516) with primers JG427 and JG428.

To assemble a constitutively expressed pVip construct to be integrated into the thrC site of *B. subtilis*, first the pVip gene was lifted from the plasmid reported in ref. [13] using primers JG3 and JG4 and Gibson assembled with a backbone amplified from plasmid pJMP4 (provided by J. M. Peters) with primers JG1 and JG2. From the resulting plasmid, pVIP was lifted with the Pveg promoter using primers JG82 and JG83 and Gibson assembled with a backbone amplified from pSG-thrC_Phspank_sfGFP using primers JG81 and OGO603.

All PCR reactions were performed using KAPA HiFi HotStart ReadyMix (Roche catalogue no. KK2601). Cloning was performed using the NEBuilder HiFi DNA Assembly kit (NEB, E2621).

***Bacillus* transformation.** Transformation to *B. subtilis* BEST7003 was performed using MC medium as previously described[25]. MC medium was composed of 80 mM K_2HPO_4, 30 mM KH_2PO_4, 2% glucose, 30 mM trisodium citrate, 22 μg ml^{-1} ferric ammonium citrate, 0.1% casein hydrolysate and 0.2% sodium glutamate. From an overnight starter of bacteria, 10 μl were diluted in 1 ml of MC medium supplemented with 10 μl of 1 mol $MgSO_4$. After 3 h of incubation (37 °C, 200 r.p.m.), 300 μl of the culture was transferred to a new 15 ml tube and ~200 ng of plasmid DNA was added. The tube was incubated for another 3 h (37 °C, 200 r.p.m.), and the entire reaction was plated on LB agar plates supplemented with 5 μg ml^{-1} chloramphenicol or 100 μg ml^{-1} spectinomycin and incubated overnight at 30 °C.

Plaque assays. Phages were propagated by picking a single phage plaque into a liquid culture of *B. subtilis* BEST7003 or *E. coli* MG1655 grown at 37 °C to OD_{600} (optical density) 0.3 in MMB medium until culture collapse. The culture was then centrifuged for 10 min at 3,200*g* and the supernatant was filtered through a 0.2 μm filter to get rid of remaining bacteria and bacterial debris. Lysate titre was determined using the small-drop plaque assay method as previously described[26].

Plaque assays were performed as previously described[6,26]. Bacteria containing a defence system and control bacteria with no system were grown overnight at 37 °C. Then, 300 μl of the bacterial culture was mixed with 30 ml melted MMB 0.5% agar, poured on 10 cm square plates, and let to dry for 1 h at room temperature. For cells that contained inducible constructs, the inducers were added to the agar before plates were poured. Tenfold serial dilutions in MMB were performed for each of the tested phages and 10 μl drops were put on the bacterial layer. After the drops had dried up, the plates were inverted and incubated overnight at room temperature or 37 °C. Plaque-forming units (PFUs) were determined by counting the derived plaques after overnight incubation, and lysate titre was determined by calculating PFUs per ml. When no individual plaques could be identified, a faint lysis zone across the drop area was considered to be 10 plaques. Details of specific conditions used in plaque assays for each defence system are found in Table 2.

Liquid culture growth assays. Non-induced overnight cultures of bacteria containing defence system and bacteria with no system (negative control) were diluted 1:100 in MMB medium supplemented with appropriate antibiotics and incubated at 37 °C while shaking at 200 r.p.m. until early log phase (OD_{600} = 0.3). 180 μl of the culture were then transferred into wells in a 96-well plate containing 20 μl of phage lysate for a final MOI of 10 and 0.1 for phage lambda(vir), an MOI of 4 and 0.04 for phages SPR, phi29 and vB_EcoM-KAW1E185, or 20 μl of MMB for uninfected control. Infections were performed in triplicates from overnight cultures prepared from separate colonies. Plates were incubated at 30 °C or 37 °C (as indicated) with shaking in a TECAN Infinite200 plate reader and an OD_{600} measurement was taken every 10 min. Details of specific conditions used for each defence system are found in Table 2.

Liquid culture growth toxicity assays. Non-induced *E. coli* MG1655 with DSR2 and tail tube, or DSR2 and RFP (negative control), were grown overnight in MMB supplemented with 1% glucose and the appropriate antibiotics. Cells were diluted 1:100 in 3 ml of fresh MMB and grown at 37 °C to an OD_{600} of 0.3 before expression was induced. The inducers were then added to a final concentration of 0.2% arabinose and 1 mM isopropyl β-D-1-thiogalactopyranoside (IPTG), and MMB was added instead for the uninduced control cells. The cells were transferred into a 96-well plate. Plates were incubated at 37 °C with shaking in a TECAN Infinite200 plate reader with an OD_{600} measurement taken every 10 min.

Infection time course phage titre assay. Non-induced overnight cultures of bacteria containing the DSR2 gene and bacteria with no system (negative control) were diluted 1:100 in 3 ml MMB medium and incubated at 37 °C while shaking at 200 r.p.m. until early log phase (OD_{600} = 0.3), and then cultures were infected with phage SPR at an MOI of 4. Cultures were left shaking at 37 °C for the duration of the experiment. At each time point, 1 ml of culture was filtered through a 0.2 μm filter (Whatman catalogue no. 10462200) and then used in an infection plaque assay on *B. subtilis* BEST7003 at room temperature. The sample for time 0 was produced by mixing the same amount of phage used for infection in 3 ml MMB medium.

Cell lysate preparation for LC-MS. Overnight cultures of bacteria containing a defence system and bacteria with no system (negative control) were diluted 1:100 in 250 ml MMB and incubated at 37 °C with shaking (200 r.p.m.) until reaching OD_{600} of 0.3. For cells that contained inducible SIR2/pAgo constructs, the inducers were added at an OD_{600} of 0.1. A sample of 50 ml of uninfected culture (time 0) was then removed, and phage stock was added to the culture to reach an MOI of 5–10. Flasks were incubated at 30 °C or 37 °C (as indicated) with shaking (200 r.p.m.) for the duration of the experiment. The 50 ml samples were collected at various time points postinfection. Immediately upon sample removal, the sample tube was placed in ice and centrifuged at 4 °C for 5 min to pellet the cells. The supernatant was discarded and the tube was frozen at −80 °C. To extract the metabolites, 600 μl of 100 mM phosphate buffer at pH 8, supplemented with 4 mg ml^{-1} lysozyme, was added to each pellet. Tubes were then incubated for 30 min at room temperature and returned to ice. The thawed sample was transferred to a FastPrep Lysing Matrix B 2 ml tube (MP Biomedicals catalogue no. 116911100) and lysed using FastPrep bead beater for 40 s at 6 m s^{-1}. Tubes were then centrifuged at 4 °C for 15 min at 15,000*g*. Supernatant was transferred to Amicon Ultra-0.5 Centrifugal Filter Unit 3 KDa (Merck Millipore catalogue no. UFC500396) and centrifuged for 45 min at 4 °C at 12,000*g*. Filtrate was taken and used for liquid chromatography mass spectrometry (LC-MS) analysis. Details of specific conditions used for each defence system are found in Table 2.

Quantification of NAD± and ADPR by LC-MS. Cell lysates were prepared as described above and analysed by LC-MS/MS. Quantification of metabolites was carried out using an Acquity I-class UPLC system coupled to Xevo TQ-S triple quadrupole mass spectrometer (both Waters, US). The UPLC was performed using an Atlantis Premier BEH C18 AX column with dimensions of 2.1 × 100 mm and particle size of 1.7 μm (Waters). Mobile phase A was 20 mM ammonium formate at pH 3, and acetonitrile was mobile phase B. The flow rate was kept at 300 μl min^{-1} consisting of a 2 min hold at 2% B, followed by linear gradient increase to 100% B over 5 min. The column temperature was set at 25 °C and an injection volume of 1 μl. An electrospray ionization interface was used as ionization source. Analysis was performed in positive ionization mode. Metabolites were detected using multiple-reaction monitoring, using argon as the collision gas. Quantification was made using standard curve in 0–1 mM concentration range. NAD+ (Sigma, N0632-1G) and ADPR (Sigma, A0752-25MG) were added to standards and samples as internal standard (0.5 μmol). TargetLynx (Waters) was used for data analysis.

Pulldown assays. Non-induced overnight cultures of *E. coli* MG1655 with DSR2 (H171A), DSAD1, DSAD1 with C-terminal TwinStrep tag, SPR tail tube protein with C-terminal TwinStrep tag, or combinations of these proteins were diluted 1:100 in 50 ml of MMB and grown at 37 °C to an OD_{600} of 0.3. Expression was then induced by adding 0.2% arabinose and 1 mM IPTG, and cells continued to grow to an OD_{600} of 0.9 at 37 °C. Cells were centrifuged at 3,200*g* for 10 min. Supernatant was discarded and pellets were frozen at −80 °C.

To pull down the proteins, 1 ml of Strep-Tactin wash buffer (IBA catalogue no. 2-1003-100) supplemented with 4 mg ml^{-1} lysozyme was added to each pellet and incubated for 10 min at 37 °C with shaking until thawed, and then resuspended. Tubes were then transferred to ice, and the resuspended cells transferred to a FastPrep Lysing Matrix B in a 2 ml tube (MP Biomedicals catalogue no. 116911100). Samples were lysed using a FastPrep bead beater for 40 s at 6 m s^{-1}. Tubes were centrifuged for 15 min at 15,000*g*. Per each pellet, 30 μl of MagStrep 'Type 3' XT beads (IBA catalogue no. 2-4090-002) were washed twice in 300 μl wash buffer (IBA catalogue no. 2-1003-100), and the lysed cell supernatant was mixed with the beads and incubated for 30–60 min, rotating at 4 °C. The beads were then pelleted on a magnet, washed twice with wash buffer, and purified protein was eluted from the beads in 10 μl of BXT elution buffer (IBA catalogue no. 2-1042-025). Some 30 μl of samples were mixed with 10 μl of 4× Bolt LDS Sample Buffer (ThermoFisher catalogue no. B0008) and a final concentration of 1 mM of dithiothreitol (DTT). Samples were incubated at 75 °C for 5 min and then loaded to a NuPAGE 4% to 12%, Bis-Tris, 1.0 mm, Mini Protein Gel, 12 well (ThermoFisher catalogue no. NP0322PK2) in 20X Bolt MES SDS Running Buffer (ThermoFisher catalogue no. B0002) and run at 160 V. Gels were shaken with InstantBlue Coomassie Protein Stain (ISB1L) (ab119211) for 1 h, followed by another hour in water. All bands shown in Fig. 3b were verified to represent the indicated protein by MS.

Phage coinfection and hybrid isolation. 50 μl overnight culture of *B. subtilis* containing DSR2 and pVip was mixed with 50 μl of phage SPR and 50 μl of either phi3T or SPbeta; each phage at a titre of 10^7 PFU ml^{-1}. Bacteria and phages were left to rest at room temperature for 10 min before being mixed with 5 ml of premelted MMB 0.3% agar and poured over a plate containing MMB 0.5% agar. Plates were left overnight at room temperature before being inspected for plaques. Single plaques were picked into 100 μl phage buffer (50 mM Tris-HCl pH 7.4, 100 mM $MgCl_2$, 10 mM NaCl). Hybrid phages were tested for their ability to infect DSR2-containing cells using small-drop plaque assay as described above.

Sequencing and assembly of phage hybrids. High-titre phage lysates (>10^7 PFUs ml^{-1}) of the ancestor and isolated phage hybrids were used for DNA extraction. A total of 500 μl of the phage lysate was treated with DNaseI (Merck catalogue no. 11284932001) added to a final concentration of 20 μg ml^{-1} and incubated at 37 °C for 1 h to remove bacterial DNA. DNA was extracted using

the QIAGEN DNeasy blood and tissue kit (catalogue no. 69504) starting from the proteinase-K treatment step to lyse the phages. Libraries were prepared for Illumina sequencing using a modified Nextera protocol as previously described[27]. Reads were de-novo assembled using Spades v.3.14.0 (ref. [28]) with the 'careful' pipeline option which reduces chances for wrong mismatches and short indels in assemblies of small genomes.

Hybrid phage alignment. Hybrid phage genomes were aligned using SnapGene v.5.3.2. Each hybrid genome was aligned to phage SPR and areas that did not align were aligned against the other phages in the co-infection experiment, to verify their origin and gene content.

Statistics and reproducibility. No statistical method was used to predetermine sample size. Experiments were performed in triplicates unless stated otherwise. Randomization was used for sample injection order in MS measurements. No data were excluded from the analyses. The experiments in Fig. 3b and Extended Data Fig. 5 were repeated independently twice with similar results.

Reporting summary. Further information on research design is available in the Nature Research Reporting Summary linked to this article.

Data availability

Data that support the findings of this study are available within the Article and its Extended Data. Gene accessions appear in the Methods section of the paper. Plasmid maps of the constructs used for the experiments are attached as Supplementary Files. Source data are provided with this paper.

Received: 15 December 2021; Accepted: 21 July 2022;
Published online: 03 October 2022

References

1. North, B. J. & Verdin, E. Protein family review Sirtuins: Sir2-related NAD-dependent protein deacetylases. *Genome Biol.* **5**, 224 (2004).
2. Imai, S., Armstrong, C. M., Kaeberlein, M. & Guarente, L. Transcriptional silencing and longevity protein Sir2 is an NAD-dependent histone deacetylase. *Nature* **403**, 795–800 (2000).
3. Tanny, J. C., Dowd, G. J., Huang, J., Hilz, H. & Moazed, D. An enzymatic activity in the yeast Sir2 protein that is essential for gene silencing. *Cell* **99**, 735–745 (1999).
4. Dang, W. & Pfizer, N. C. The controversial world of sirtuins. *Drug Discov. Today Technol.* **12**, e9–e17 (2014).
5. Makarova, K. S., Wolf, Y. I., van der Oost, J. & Koonin, E. V. Prokaryotic homologs of Argonaute proteins are predicted to function as key components of a novel system of defense against mobile genetic elements. *Biol. Direct* **4**, 29 (2009).
6. Doron, S. et al. Systematic discovery of antiphage defense systems in the microbial pangenome. *Science* **359**, eaar4120 (2018).
7. Ofir, G. et al. Antiviral activity of bacterial TIR domains via signaling molecules that trigger cell death. *Nature* **600**, 116–120 (2021).
8. Gao, L. et al. Diverse enzymatic activities mediate antiviral immunity in prokaryotes. *Science* **369**, 1077–1084 (2020).
9. Lopatina, A., Tal, N. & Sorek, R. Abortive infection: Bacterial suicide as an antiviral immune strategy. *Annu. Rev. Virol.* **7**, 371–384 (2020).
10. Kohm, K. & Hertel, R. The life cycle of SPβ and related phages. *Arch. Virol.* **166**, 2119–2130 (2021).
11. Noyer-Weidner, M., Jentsch, S., Pawlek, B., Günthert, U. & Trautner, T. A. Restriction and modification in *Bacillus subtilis*: DNA methylation potential of the related bacteriophages Z, SPR, SP beta, phi 3T, and rho 11. *J. Virol.* **46**, 446–453 (1983).
12. Dragoš, A. et al. Pervasive prophage recombination occurs during evolution of spore-forming Bacilli. *ISME J.* **15**, 1344–1358 (2021).
13. Bernheim, A. et al. Prokaryotic viperins produce diverse antiviral molecules. *Nature* **589**, 120–124 (2021).
14. Freire, D. M. et al. An NAD+ phosphorylase toxin triggers mycobacterium tuberculosis cell death. *Mol. Cell* **73**, 1282–1291.e8 (2019).
15. Morehouse, B. R. et al. STING cyclic dinucleotide sensing originated in bacteria. *Nature* **586**, 429–433 (2020).
16. Skjerning, R. B., Senissar, M., Winther, K. S., Gerdes, K. & Brodersen, D. E. The RES domain toxins of RES-Xre toxin-antitoxin modules induce cell stasis by degrading NAD. *Mol. Microbiol.* **111**, 221–236 (2019).
17. Tang, J. Y., Bullen, N. P., Ahmad, S. & Whitney, J. C. Diverse NADase effector families mediate interbacterial antagonism via the type VI secretion system. *J. Biol. Chem.* **293**, 1504–1514 (2018).
18. Tal, N. et al. Cyclic CMP and cyclic UMP mediate bacterial immunity against phages. *Cell* **184**, 5728–5739.e16 (2021).
19. Millman, A. et al. Bacterial retrons function in anti-phage defense. *Cell* **183**, 1551–1561.e12 (2020).
20. Kaufmann, G. Anticodon nucleases. *Trends Biochem. Sci.* **25**, 70–74 (2000).
21. Depardieu, F. et al. A eukaryotic-like serine/threonine kinase protects staphylococci against phages. *Cell Host Microbe* **20**, 471–481 (2016).
22. Millman, A. et al. An expanding arsenal of immune systems that protect bacteria from phages. Preprint at *bioRxiv* https://doi.org/10.1101/2022.05.11.491447 (2022).
23. Cohen, D. et al. Cyclic GMP–AMP signalling protects bacteria against viral infection. *Nature* **574**, 691–695 (2019).
24. Overkamp, W. et al. Benchmarking various green fluorescent protein variants in *Bacillus subtilis*, *Streptococcus pneumoniae*, and *Lactococcus lactis* for live cell imaging. *Appl. Environ. Microbiol.* **79**, 6481–6490 (2013).
25. Wilson, G. A. & Bott, K. F. Nutritional factors influencing the development of competence in the *Bacillus subtilis* transformation system. *J. Bacteriol.* **95**, 1439–1449 (1968).
26. Mazzocco, A., Waddell, T. E., Lingohr & E, J. R. Enumeration of bacteriophages using the small drop plaque assay system. *Methods Mol. Biol.* **501**, 81–85 (2009).
27. Baym, M. et al. Inexpensive multiplexed library preparation for megabase-sized genomes. *PLoS ONE* **10**, e0128036 (2015).
28. Prjibelski, A., Antipov, D., Meleshko, D., Lapidus, A. & Korobeynikov, A. Using SPAdes De Novo Assembler. *Curr. Protoc. Bioinforma.* **70**, 1–29 (2020).
29. Gilchrist, C. L. M. & Chooi, Y.-H. Clinker & Clustermap.Js: automatic generation of gene cluster comparison figures. *Bioinformatics* **37**, 2473–2475 (2021).
30. Gabler, F. et al. Protein sequence analysis using the MPI bioinformatics toolkit. *Curr. Protoc. Bioinforma.* **72**, 1–30 (2020).
31. Zaremba, M. et al. Sir2-domain associated short prokaryotic Argonautes provide defence against invading mobile genetic elements through NAD+ depletion. Preprint at *bioRxiv* https://doi.org/10.1101/2021.12.14.472599 (2021).
32. Altschul, S. F. et al. Gapped BLAST and PSI-BLAST: a new generation of protein database search programs. *Nucleic Acids Res.* **25**, 3389–3402 (1997).

Acknowledgements

We thank the Sorek laboratory members for comments on the manuscript and fruitful discussion. We also thank A. Brandis and T. Mehlman from the Weizmann Life Sciences Core Facilities for targeted mass spectrometry analyses, and A. Savidor from the Israel National Center for Personalized Medicine for protein mass spectrometry. R.S. was supported, in part, by the European Research Council (grant nos. ERC-CoG 681203 and ERC-AdG GA 101018520), Israel Science Foundation (grant no. ISF 296/21), the Ernest and Bonnie Beutler Research Program of Excellence in Genomic Medicine, the Deutsche Forschungsgemeinschaft (SPP 2330, grant no. 464312965), the Minerva Foundation with funding from the Federal German Ministry for Education and Research and the Knell Family Centre for Microbiology. V.S. was supported by the European Social Fund (grant no. 09.3.3-LMT-K-712-01-0126) under a grant agreement with the Research Council of Lithuania (LMTLT).

Author contributions

J.G. and R.S. led the study and performed all analyses and experiments unless otherwise indicated. A. Lopatina performed plaque assay experiments with the SIR2/pAgo defence system. A.B. cloned and conducted plaque assays for the pVip defence system. M.Z. and V.S. provided the SIR2/pAgo defence system. S.M. and A. Leavitt cloned and conducted plaque assays for the DSR2, DSR1 and SIR2-HerA defence systems. A.M. and G.A. assisted with sequence analysis and prediction of protein domain functions and point mutations. The manuscript was written by J.G. and R.S. All authors contributed to editing the manuscript, and support the conclusions.

Competing interests

R.S. is a scientific cofounder and advisor of BiomX and Ecophage. The other authors declare no competing interests.

Additional information

Extended data is available for this paper at https://doi.org/10.1038/s41564-022-01207-8.

Supplementary information The online version contains supplementary material available at https://doi.org/10.1038/s41564-022-01207-8.

Correspondence and requests for materials should be addressed to Rotem Sorek.

Peer review information *Nature Microbiology* thanks Lennart Randau, Malcolm White and the other, anonymous, reviewer(s) for their contribution to the peer review of this work.

Reprints and permissions information is available at www.nature.com/reprints.

Publisher's note Springer Nature remains neutral with regard to jurisdictional claims in published maps and institutional affiliations.

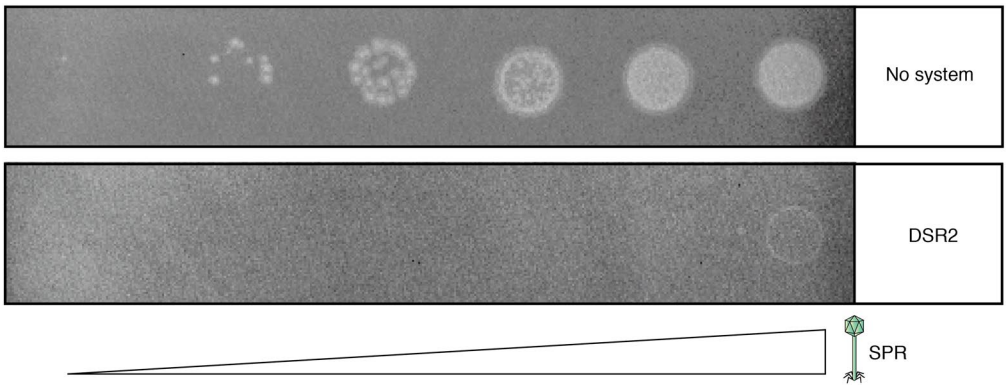

Extended Data Fig. 1 | Exemplary plaque assay results showing DSR2 defence. Plaque assay with tenfold serial dilution of phage SPR on the control *B. subtilis* strain (no system) or *B. subtilis* with DSR2.

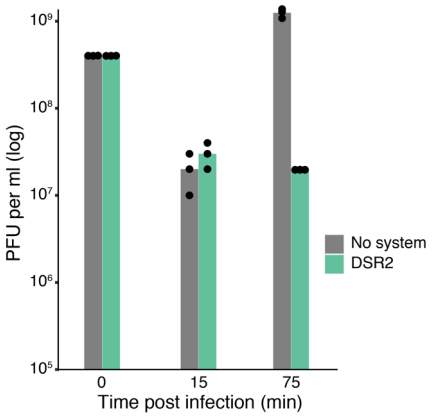

Extended Data Fig. 2 | Phage SPR does not replicate in high MOI infection of DSR2-containing cells. Titre of phage SPR at different time points following infection of the control *B. subtilis* strain (no system) or *B. subtilis* with DSR2. Data represent plaque-forming units (PFU) per millilitre. Bar graphs represent average of three independent replicates, with individual data points overlaid.

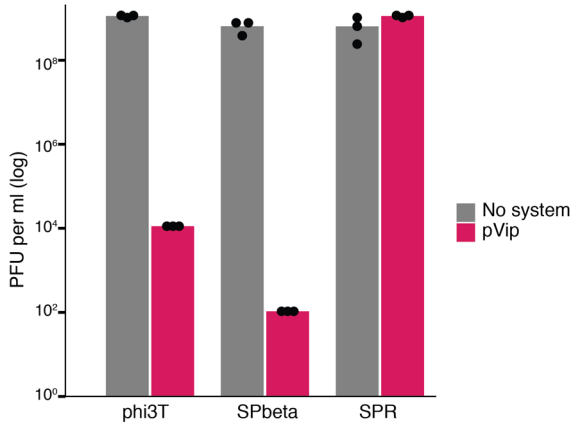

Extended Data Fig. 3 | pVip alone protects against phi3T and SPbeta but not against SPR. Efficiency of plating (EOP) for three phages infecting the control *B. subtilis* strain (no system) or *B. subtilis* with pVip cloned from *Fibrobacter sp.* UWT3. Data represent plaque-forming units (PFU) per millilitre. Bar graphs represent average of three independent replicates, with individual data points overlaid. Control data are the same as those presented in Fig. 1b.

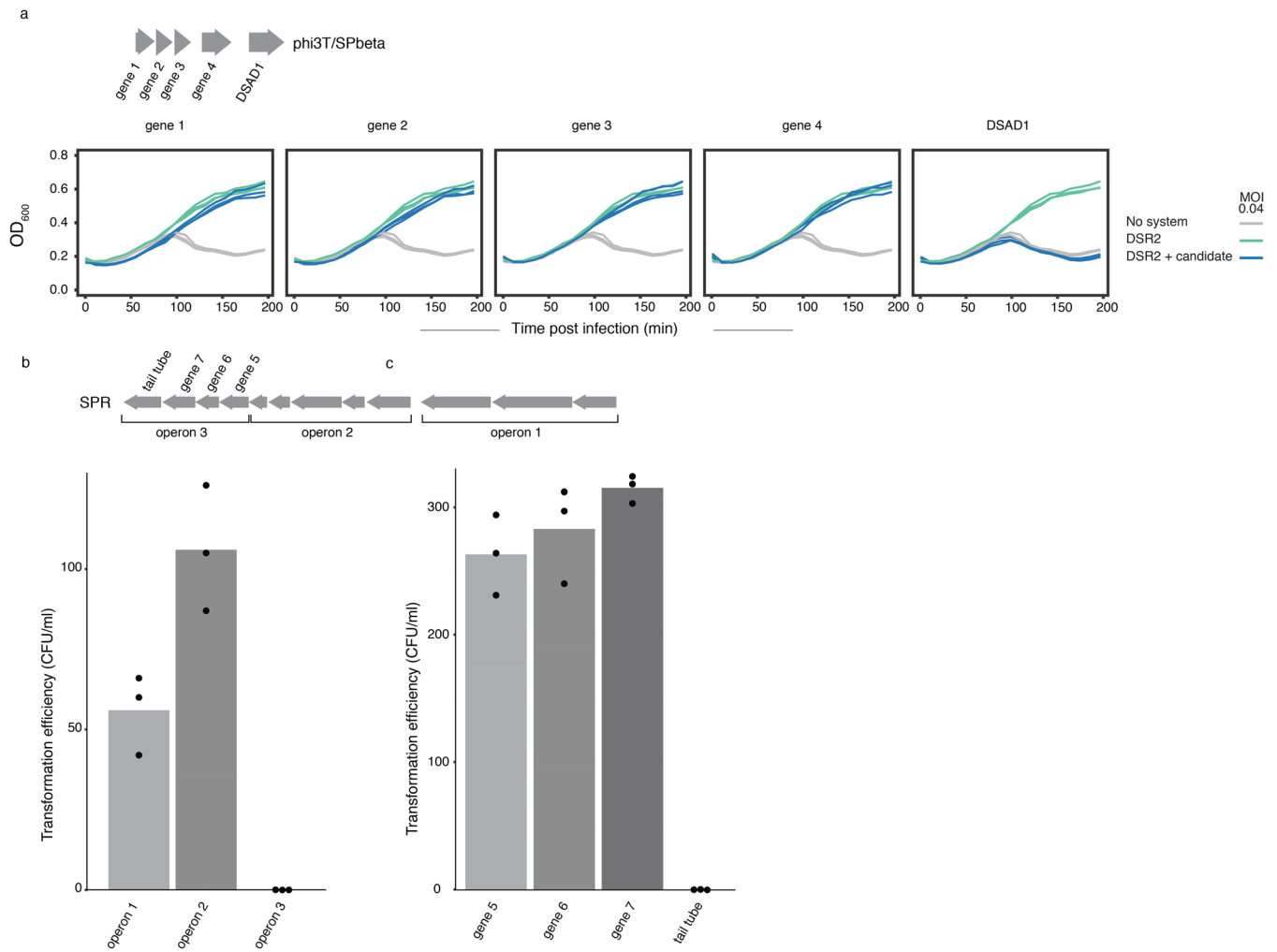

Extended Data Fig. 4 | Testing of candidate genes for inhibition and activation of DSR2. Legend of genes and operons tested included above. (**a**) Liquid culture growth of *B. subtilis* BEST7003 cells expressing either DSR2 alone, or DSR2 and a candidate gene, or control cells expressing neither gene, infected by phage SPR at 30 °C. Bacteria were infected at time 0 at an MOI of 0.04. Three independent replicates are shown for each MOI, and each curve shows an individual replicate. Each panel shows a different candidate gene. The 'No system' and the DSR2 control curves are the same for all 5 panels. (**b**, **c**) Transformation efficiencies of a vector containing operon 1-3 (panel B), or 4 individual genes from operon 3 (panel C) were measured for cells containing WT DSR2. Y axis represents the number of colony-forming units per millilitre obtained following transformation. Bar graphs represent average of three replicates, with individual data points overlaid.

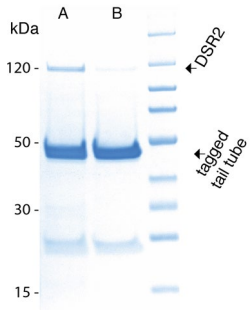

Extended Data Fig. 5 | The tail tube does not pull down DSR2 when DSAD1 is co-expressed. Pulldown assays of the DSR2-tail tube complex, heterologously expressed in *E. coli*. The tail tube protein of phage SPR was C-terminally tagged with TwinStrep tag. DSR2 in this experiment was mutated (H171A) to avoid toxicity. Shown is an SDS-PAGE gel. Lane A, cells expressing tagged tail tube protein from SPR, DSR2 (H171A) and GFP. Lane B, cells expressing tagged tail tube protein from SPR, DSR2 (H171A) and DSAD1.

Extended Data Fig. 6 | Multiple sequence alignment comparing the tail tube protein of SPR and SPbeta/phi3T. The NCBI accessions for the SPR and phi3T/SPbeta tail tube proteins are WP_010328117 and WP_004399252, respectively (the phi3T tail tube protein is identical to that of SPbeta). Protein amino acid sequences were aligned by Clustal Omega[30].

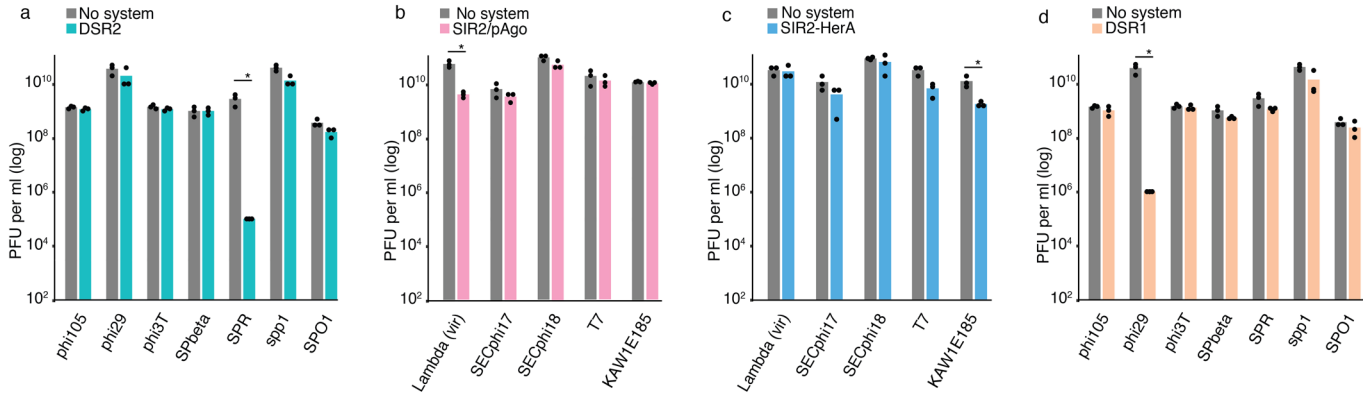

Extended Data Fig. 7 | SIR2-containing defence systems protect against multiple phages. a-d. Efficiency of plating (EOP) for multiple phages infecting control bacteria (no system) or bacteria expressing defence systems. Data represent plaque-forming units (PFU) per millilitre. Bar graphs represent average of three independent replicates, with individual data points overlaid. KAW1E185 is short for vB_EcoM-KAW1E185, a T4-like phage. Data appearing in this figure also appear in Fig. 4b. Data for control samples are the same in panels A and D. Asterisk marks statistically significant decreases (Student's t-test, two-sided, *P* values = 0.020, 0.005, 0.036, 0.014, for phages SPR with DSR2, lambda (vir) with SIR2/pAgo, KAW1E185 with SIR2-HerA, phi29 with DSR1, respectively).

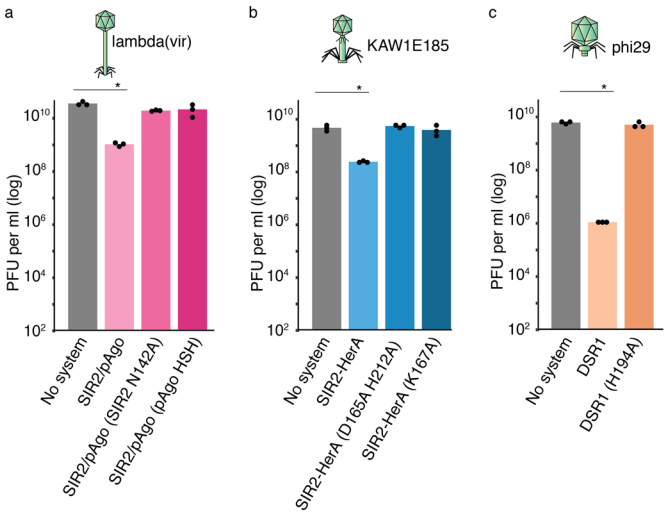

Extended Data Fig. 8 | Testing for defence in mutants of SIR2/pAgo, SIR2-HerA and DSR1. a-c. Efficiency of plating (EOP) for phages infecting the control strain (no system), bacteria containing the WT defence system, and bacteria containing mutants of the defence system. In all cases except for pAgo, point mutations were introduced in the predicted active site of the protein. For the pAgo, a bulky HSH tag, which was shown in another study to inactivate the protein[31], was added to the C-terminus. Data represent plaque-forming units (PFU) per millilitre. Bar graphs represent average of three independent replicates, with individual data points overlaid. Asterisk marks statistically significant decreases (Student's t-test, two-sided, *P* values = <0.001, 0.002, <0.001, for phages lambda (vir) with SIR2/pAgo, KAW1E185 with SIR2-HerA, phi29 with DSR1, respectively).

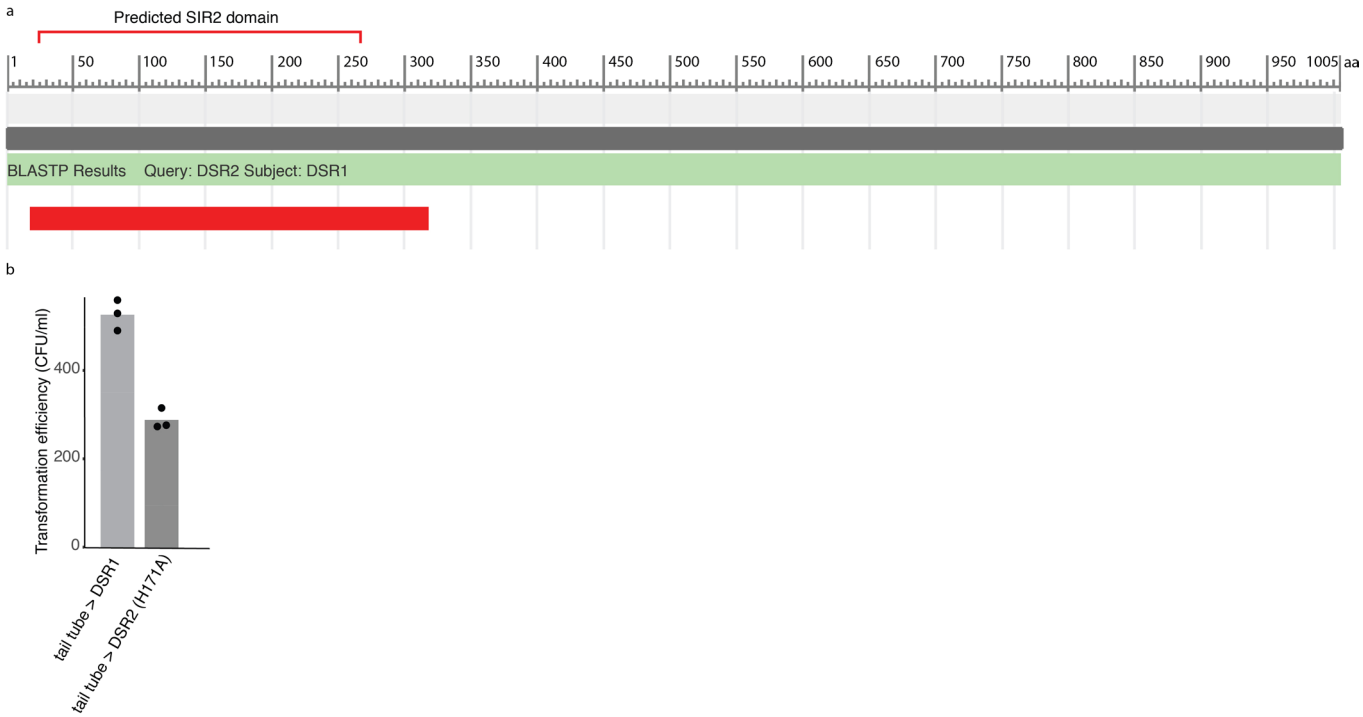

Extended Data Fig. 9 | DSR1 and DSR2 alignment is limited to the SIR2 domain. SPR tail tube does not activate DSR1. (**a**) Graphical representation of running BLASTP[32] with a query of DSR2 and subject of DSR1. The red area spans an alignment with 23.29% identity and an E value of 9e-07. The rest of the protein is not alignable. The red bracket above indicates the predicted SIR2 domain. (**b**) Transformation efficiencies of a vector containing the SPR tail tube protein were measured for cells containing either DSR1 or an inactive DSR2 mutant (H171A) as control. The *y* axis represents the number of colony-forming units per millilitre. Bar graphs represent average of three replicates, with individual data points overlaid.

nature portfolio

Corresponding author(s): Rotem Sorek

Last updated by author(s): Jul 11, 2022

Reporting Summary

Nature Portfolio wishes to improve the reproducibility of the work that we publish. This form provides structure for consistency and transparency in reporting. For further information on Nature Portfolio policies, see our Editorial Policies and the Editorial Policy Checklist.

Statistics

For all statistical analyses, confirm that the following items are present in the figure legend, table legend, main text, or Methods section.

n/a	Confirmed
☐	☒ The exact sample size (*n*) for each experimental group/condition, given as a discrete number and unit of measurement
☐	☒ A statement on whether measurements were taken from distinct samples or whether the same sample was measured repeatedly
☐	☒ The statistical test(s) used AND whether they are one- or two-sided *Only common tests should be described solely by name; describe more complex techniques in the Methods section.*
☒	☐ A description of all covariates tested
☒	☐ A description of any assumptions or corrections, such as tests of normality and adjustment for multiple comparisons
☒	☐ A full description of the statistical parameters including central tendency (e.g. means) or other basic estimates (e.g. regression coefficient) AND variation (e.g. standard deviation) or associated estimates of uncertainty (e.g. confidence intervals)
☐	☒ For null hypothesis testing, the test statistic (e.g. *F*, *t*, *r*) with confidence intervals, effect sizes, degrees of freedom and *P* value noted *Give P values as exact values whenever suitable.*
☒	☐ For Bayesian analysis, information on the choice of priors and Markov chain Monte Carlo settings
☒	☐ For hierarchical and complex designs, identification of the appropriate level for tests and full reporting of outcomes
☒	☐ Estimates of effect sizes (e.g. Cohen's *d*, Pearson's *r*), indicating how they were calculated

Our web collection on statistics for biologists contains articles on many of the points above.

Software and code

Policy information about availability of computer code

Data collection	Plate reader data was collected using a Tecan Infinite 200 instrument with Tecan iControl v3.8.2.0 software.
Data analysis	SnapGene Version 5.3.2. Spades3.14.0 Clustal-Omega (version 1.2.4) BLAST+ 2.13.0 TargetLynx (version 4.2)

For manuscripts utilizing custom algorithms or software that are central to the research but not yet described in published literature, software must be made available to editors and reviewers. We strongly encourage code deposition in a community repository (e.g. GitHub). See the Nature Portfolio guidelines for submitting code & software for further information.

Data

Policy information about availability of data

All manuscripts must include a data availability statement. This statement should provide the following information, where applicable:

- Accession codes, unique identifiers, or web links for publicly available datasets
- A description of any restrictions on data availability
- For clinical datasets or third party data, please ensure that the statement adheres to our policy

Data that support the findings of this study are available within the Article and its Extended Data. Gene accessions appear in the Methods section of the paper. Plasmid maps of the constructs used for the experiments are attached as Supplementary Files. Source data are provided with this paper.

Field-specific reporting

Please select the one below that is the best fit for your research. If you are not sure, read the appropriate sections before making your selection.

☒ Life sciences ☐ Behavioural & social sciences ☐ Ecological, evolutionary & environmental sciences

For a reference copy of the document with all sections, see nature.com/documents/nr-reporting-summary-flat.pdf

Life sciences study design

All studies must disclose on these points even when the disclosure is negative.

Sample size	Experiments were performed in triplicates without prior sample size calculation, as is standard for such experimental designs.
Data exclusions	No data was excluded
Replication	Experiments were performed in triplicates as is standard for such experimental designs. No failed replications occurred.
Randomization	Randomization was used for sample injection order in mass spectrometry measurements. Randomization is not standard for the other experiments performed.
Blinding	Blinding is not standard for the experiments performed

Reporting for specific materials, systems and methods

We require information from authors about some types of materials, experimental systems and methods used in many studies. Here, indicate whether each material, system or method listed is relevant to your study. If you are not sure if a list item applies to your research, read the appropriate section before selecting a response.

Materials & experimental systems

n/a	Involved in the study
☒	☐ Antibodies
☒	☐ Eukaryotic cell lines
☒	☐ Palaeontology and archaeology
☒	☐ Animals and other organisms
☒	☐ Human research participants
☒	☐ Clinical data
☒	☐ Dual use research of concern

Methods

n/a	Involved in the study
☒	☐ ChIP-seq
☒	☐ Flow cytometry
☒	☐ MRI-based neuroimaging